

# Improving GNSS Attitude Determination

Using Inertial and Magnetic Field Sensors



Determination of horizontal attitude poses a general problem for navigation applications, especially those using small aerial platforms and requiring low-cost solutions. A team of German engineers are exploring a method that combines accelerometers, gyroscopes, and a magnetic field sensor with a GNSS compass to provide a multi-sensor attitude system for portable, small-sized launcher applications. Constraints applied within an extended LAMBDA method result in a shortened time to first fix and increased reliability of the ambiguity resolution. Other promising results include bridging GNSS dropouts as well as enhanced integrity monitoring.

**JOCHEN ROTH**

KARLSRUHE INSTITUTE OF TECHNOLOGY, GERMANY

**CLAUS KASCHWICH**

TECHNISCHE UNIVERSITÄT BRAUNSCHWEIG, GERMANY

**GERT F. TROMMER**

KARLSRUHE INSTITUTE OF TECHNOLOGY, GERMANY

**T**his article describes an integration of a single-frequency GNSS, two-antenna heading system with low-cost inertial and magnetic field sensors in order to improve the availability and reliability of pure GNSS attitude determination. This method calculates a redundant attitude solution in an error-state Kalman filter using different sensor setups. As a result, the process of carrier phase ambiguity resolution accelerates.

Our approach exploits the known baseline length and an estimation of the inertial yaw and pitch angles are exploited in an extension of the LAMBDA method for a significant reduction in the ambiguity search. This not only reduces the time to first fix (TFFF) but also increases the reliability of the fixed ambiguities. With regard to small-sized and portable launcher applications, we emphasize a leveled system structure and short baseline lengths of up to 20 centimeters.



Measurement results demonstrate that our system enables single-epoch ambiguity resolution. The existence of the precise GNSS heading information facilitates an online calibration of magnetic field sensors. In turn, a calibrated magnetic field sensor enables the recovering of heading information during GNSS outages without any loss of accuracy.

### **The Challenge of Attitude Determination**

Determination of horizontal attitude poses a general problem for navigation applications. Whereas roll and pitch angles can be calculated from accelerometer measurements of the gravity vector, the yaw angle is poorly observable, especially during periods of low platform dynamics. Aiding with a magnetic field sensor is possible, but such measurements suffer from systematic magnetic deviation errors.

A GNSS compass, however, provides attitude information unafflicted by any systematic offset errors. With an array of at least three antennas, the entire orientation of the antenna structure can be determined. The necessary accuracy, even for short antenna baselines in the sub-meter range, is gained by carrier phase processing. However, this entails additional complexity due to the required

resolution of carrier phase ambiguities.

A widespread technique to identify carrier phase ambiguities is the LAMBDA (Least-squares AMBiguity Decorrelation Adjustment) method described in the article by P. Teunissen listed in the Additional Resources section near the end of this article.). Using a floating estimation of the ambiguities and the corresponding variance matrix, we can solve the integer least-squares problem in a very efficient way, achieving dual-frequency data resolution within a few observation epochs. However, real-time ambiguity resolution based on data from low-cost, single-frequency GNSS receivers is not readily possible. Employing relative positioning, however, introduces new opportunities because additional information can be provided. A reduction of the ambiguity search space is accomplished by accounting for the known baseline length (For details, see the articles by P. Clark *et alia* and R. Mönikes *et alia* 2005 listed

in Additional Resources). As a result, real-time resolution of double-differenced ambiguities from single-frequency data is possible.

For a further acceleration of the ambiguity identification process, an extension of the LAMBDA algorithm has been proposed (Mönikes *et alia* 2007) to enable a seamless integration of yaw and pitch angle constraints in the LAMBDA method, which in turn yields an additional shortening of the time to first fix.

In this article, we describe our combination of a single-frequency GNSS compass with low-cost inertial and magnetic field sensors to test this approach. With regard to launcher applications where leveled system alignment can be assured, we use a two-antenna system with a fixed baseline length of 20 centimeters. Hence, the GNSS attitude solution only consists of heading (yaw angle) and elevation (pitch angle) information.

Using inertial sensor data, redundant attitude estimation is carried out in an error-state Kalman filter which can be exploited as yaw and pitch angle constraints in the Extended LAMBDA method proposed by Mönikes *et alia*. Besides the reduction in the time to first fix, another benefit accrues from the creation of a redundant attitude solution. Where a pure GNSS attitude system would fail during signal outages, the redundant inertial attitude could bridge short periods of time and therefore form a more reliable attitude determination system.

In the next section, we briefly introduce the algorithmic basis of our system, namely the Extended LAMBDA method. Thereafter, we present the inertial attitude filter with its system and measurement models. Subsequent discussion illustrates the fusion of both independent attitude determination systems is illustrated. After presenting test results, we will describe possible system refinements, including aspects of integrity monitoring and an online calibration of the magnetic field sensor.

### **Extended LAMBDA Method**

With measurements from two receivers and creation of wide-lane combinations, the LAMBDA algorithm can provide ambiguity resolution within a few epochs. However, for L1 carrier phase measurements with its short wavelength of 19 centimeters, instantaneous ambiguity fixing cannot be accomplished by the original LAMBDA method. As mentioned earlier, Mönikes *et alia* proposed one possible solution in a 2005 article by introducing an advancement of the LAMBDA algorithm for relative positioning.

For a fixed system structure the baseline length can be assumed as known. Furthermore, some GNSS compass applications allow for restrictions concerning potential attitude angles. For example, expected pitch angles for ships or trains are small. The Extended LAMBDA method enables one to account for constraints with the aim of a further reduction in the ambiguity search space. In other words, we only investigate those combinations of ambiguities leading to a base vector consistent with the constraints.

As the ambiguity search space consists of the multidimensional ambiguity domain, the given constraints in the three-

dimensional position domain can only be applied for three primary ambiguities. From the model of the double-differenced carrier phase

$$\phi_{dd} = \frac{(\vec{e}_i^T - \vec{e}_j^T)}{\lambda} \vec{r} + N_{dd,int} \quad (1)$$

with the unit vector to satellite  $i$ ,  $\vec{e}_i^T$ ; the carrier wavelength,  $\lambda$ ; and the double-differenced integer ambiguity,  $N_{dd,int}$ , the base vector  $\vec{r}$  based on three primary ambiguities (index  $p$ ) can be formulated in matrix notation as:

$$\vec{r}_p = \mathbf{H}_p^{-1} (\vec{\phi}_{dd,p} - \vec{N}_{dd,int,p}) \quad (2)$$

In order to achieve the most accurate estimation, we base the selection of the three primary measurements on the lowest dilution of precision (DOP) as a measure of beneficial satellite geometry.

**Baseline Length Constraint.** With the given baseline length,  $l$ , the constraint for the baseline length is defined by:

$$l^2 = \|\vec{r}\|^2 = \vec{r}^T \vec{r} \quad (3)$$

Taking into account an error in the carrier phase measurements that yields a variation of the estimated baseline length of  $\pm \Delta l$ , the inequality

$$\begin{aligned} (l - \Delta l)^2 &\leq \\ (\vec{\phi}_{dd,p} - \vec{N}_{dd,int,p})^T \mathbf{H}_p^{-1,T} \mathbf{H}_p^{-1} (\vec{\phi}_{dd,p} - \vec{N}_{dd,int,p}) &\leq (l + \Delta l)^2 \end{aligned} \quad (4)$$

can be formulated from (2) and (3). This mathematical condition reduces the search space of the three primary ambiguities to a spherical shell.

In order to embed the inequality [Equation (4)] in the sequential processing steps of the LAMBDA method, we apply a Cholesky decomposition of the square and positive-definite matrix,  $\mathbf{H}_p^{-1,T} \mathbf{H}_p^{-1}$ . Similar to the deviation of the LAMBDA equations, it allows the definition of recursive limits for every single ambiguity.

**Yaw and Pitch Angle Constraints.** The formulation of an equation for attitude angle constraints is based on the orthogonal projection of the normalized base vector. With the unit vector  $\vec{e}_{up}$  pointing in the up direction, the pitch angle  $\theta$  can be calculated by:

$$\sin \theta = \frac{\vec{e}_{up}^T \cdot \vec{r}}{\|\vec{r}\|} \quad (5)$$

With an estimation of the actual pitch angle,  $\theta_0$ , and the known baseline length,  $l$ , as well as an allowed range,  $\Delta \theta$  and  $\Delta l$ , respectively, a condition for the orthogonal projection can be formulated:

$$|\vec{e}_{up}^T \cdot \vec{r}| \leq |(l + \Delta l) \sin(\theta_0 \pm \Delta \theta)| \quad (6)$$

Inserting Equation (2) with  $\rho_p = (\vec{\phi}_{dd,p} - \vec{N}_{dd,int,p})$  into Equation (6) results in

$$|a_1 \rho_1 + a_2 \rho_2 + a_3 \rho_3| \leq |(l \pm \Delta l) \sin(\theta_0 \pm \Delta \theta)| \quad (7)$$

$\mathbf{H}_{p,i}^{-1}$  is the definition of the  $i$ th column of the matrix  $\mathbf{H}_p^{-1}$ . Consequently, the coefficients  $a_i$  in Equation (7) hold:

$$a_i = \vec{e}_{up}^T \mathbf{H}_{p,i}^{-1} \quad (8)$$

Since the signs of the coefficients,  $a_p$ , are unknown, only a limit for the third ambiguity (included in  $\rho_3$ ) can be defined. This results in the following conditions:

$$\begin{aligned} & \frac{-|R_1 \sin(\theta_0 - \Delta \theta)| - (a_1 \rho_1 + a_2 \rho_2)}{a_3} \\ & \leq \rho_3 \leq \frac{|R_2 \sin(\theta_0 + \Delta \theta)| - (a_1 \rho_1 + a_2 \rho_2)}{a_3} \end{aligned} \quad (9)$$

if  $a_3 > 0$

and

$$\begin{aligned} R_1 &= l + \Delta l \quad \text{if } \theta_0 - \Delta \theta < 0 \\ R_1 &= l - \Delta l \quad \text{if } \theta_0 - \Delta \theta \geq 0 \\ R_2 &= l - \Delta l \quad \text{if } \theta_0 + \Delta \theta < 0 \\ R_2 &= l + \Delta l \quad \text{if } \theta_0 + \Delta \theta \geq 0 \end{aligned} \quad (10)$$

In order to determine constraints for the yaw angle instead of  $\vec{e}_{up}$ , we use a unit vector in the body-y direction

$$\vec{e}_y = (\sin \psi_0, \cos \psi_0, 0)^T \quad (11)$$

Thereby  $\psi_0$  is the actual yaw angle. The rest of the derivation is similar to the earlier analysis. For the sake of completeness, the implemented inequalities for attitude constraints are:

$$\begin{aligned} & \frac{-|(l + \Delta l) \sin \Delta \psi| - (a_1 \rho_1 + a_2 \rho_2)}{a_3} \\ & \leq \rho_3 \leq \frac{|(l + \Delta l) \sin \Delta \psi| - (a_1 \rho_1 + a_2 \rho_2)}{a_3} \end{aligned} \quad (12)$$

if  $a_3 > 0$  and

$$\begin{aligned} & \frac{-|(l + \Delta l) \sin \Delta \psi| - (a_1 \rho_1 + a_2 \rho_2)}{a_3} \\ & \geq \rho_3 \geq \frac{|(l + \Delta l) \sin \Delta \psi| - (a_1 \rho_1 + a_2 \rho_2)}{a_3} \end{aligned}$$

if  $a_3 < 0$ .

To reject the region of  $\psi_0 + \Delta \psi + 180^\circ$ , the condition

$$\frac{-(a_1 \rho_1 + a_2 \rho_2)}{a_3} \leq \rho_3 \quad \text{if } a_3 > 0 \quad (13)$$

$$\frac{-(a_1 \rho_1 + a_2 \rho_2)}{a_3} \geq \rho_3 \quad \text{if } a_3 < 0$$

must also be fulfilled.

The extension of the LAMBDA method that we have described here forms the algorithmic base of our improved atti-

tude determination system. It enables seamless integration of attitude constraints in the highly efficient LAMBDA algorithm. Hereby, not only the time to first fix can be abbreviated but also the reliability is enhanced as the reduction of the ambiguity search space excludes potential wrong fixes.

## Inertial Attitude Filtering

While it is conceivable to assume a static pitch angle constraint for some applications (e.g., ships and trains), utilizing yaw angle constraints are only realizable with external sensor information. For this purpose, we designed an inertial attitude determination system consisting of gyroscopes, accelerometers, and a magnetic field sensor.

In order to determine an attitude solution, yaw, pitch, and roll angles are propagated in a strapdown algorithm using gyroscope measurements with an update rate of 265 hertz. Due to the inherent bias of gyroscope sensors, this solution would be prone to large errors in a very short time. Therefore, an error-state Kalman filter is implemented. The state vector comprises attitude errors and errors of the gyroscope sensor bias estimates:

$$\tilde{x} = (\alpha, \beta, \gamma, \Delta b_{\omega, x}, \Delta b_{\omega, y}, \Delta b_{\omega, z})^T = (\Delta \tilde{\psi}, \Delta \tilde{b}_{\omega})^T \quad (14)$$

Neglecting the influences of Earth's rate and Coriolis force, the system model is given by:

$$\begin{pmatrix} \dot{\Delta \tilde{\psi}} \\ \dot{\Delta \tilde{b}_{\omega}} \end{pmatrix} = \begin{pmatrix} \mathbf{0} & \hat{\mathbf{C}}_b^n \\ \mathbf{0} & \mathbf{0} \end{pmatrix} \begin{pmatrix} \Delta \tilde{\psi} \\ \Delta \tilde{b}_{\omega} \end{pmatrix} + \begin{pmatrix} \hat{\mathbf{C}}_b^n & \mathbf{0} \\ \mathbf{0} & \mathbf{I} \end{pmatrix} \begin{pmatrix} \tilde{n}_{\omega} \\ \tilde{n}_{b_{\omega}} \end{pmatrix} \quad (15)$$

with the estimated direction cosine matrix,  $\hat{\mathbf{C}}_b^n$ , used to transform the body-frame into the navigation-frame, the measurement noise of the gyroscope sensors,  $\tilde{n}_{\omega}$ , and the noise of the gyroscope sensor biases,  $\tilde{n}_{b_{\omega}}$ .

The aiding of roll and pitch angles in the Kalman filter is provided by accelerometer measurements. For applications with moderate dynamics, these measurements are dominated by the local gravity vector. Hence, the accelerometer measurement model holds:

$$\tilde{a}_{ib}^b = -\hat{\mathbf{C}}_b^{n,T} \tilde{g}_l^n + \tilde{n}_a \quad (16)$$

with gravity vector,  $\tilde{g}_l^n = (0, 0, g)^T$ . In this case,  $\tilde{n}_a$  not only accounts for the accelerometer measurement noise but also influences of the unmodeled trajectory dynamics.

With the relationship between the true and estimated direction cosine matrix

$$\mathbf{C}_b^{n,T} = \hat{\mathbf{C}}_b^{n,T} (\mathbf{I} - \Psi) \quad (17)$$

where  $\Psi$  denotes the skew symmetric matrix of the attitude errors, the final model equation is given by:

$$\tilde{a}_{ib}^b + \hat{\mathbf{C}}_b^{n,T} \tilde{g}_l^n = -\hat{\mathbf{C}}_b^{n,T} \begin{pmatrix} 0 & -g \\ g & 0 \\ 0 & 0 \end{pmatrix} \begin{pmatrix} \alpha \\ \beta \end{pmatrix} + \tilde{n}_a \quad (18)$$

From Equation (18) it becomes apparent that the yaw angle error is not observable by means of accelerometer measurements. Without additional aiding by data from a magnetic field sensor, this error would grow unchecked.

The extraction of yaw angle information from measurements of magnetic field sensors requires additional information. On the one hand, the local magnetic field vector in coordinates of the navigation-frame

$$\tilde{h}^n = (h_n, h_e, h_d)^T \quad (19)$$

must be known and can be calculated on the basis of approximate position and time using the World Magnetic Model (WMM) (see NOAA in Additional Resources). On the other hand, the extraction of heading information from the measured magnetic field requires the knowledge of horizontal alignment, i.e., roll and pitch angles.

By using an attitude filter, roll and pitch angle estimates are available. The measurement model describes the relationship of the measured magnetic field in coordinates of the body-frame to the given local magnetic field in the navigation frame, i.e.,

$$\tilde{h}^b = \mathbf{C}_b^{n,T} \tilde{h}^n + \tilde{v}_m \quad (20)$$

where  $\tilde{v}_m$  is the measurement noise.

Substituting Equation (17) into Equation (20) leads to the measurement model

$$\tilde{h}^b - \hat{\mathbf{C}}_b^{n,T} \tilde{h}^n = \hat{\mathbf{C}}_b^{n,T} [\tilde{h}^n \times] \tilde{\psi} + \tilde{v}_m \quad (21)$$

Unlike the accelerometer measurements, all three attitude angles are now observable. However, because of larger errors, magnetic field measurements are only used for yaw angle updates. Measurements of the accelerometer provide a more reliable aiding for roll and pitch angles. This simplifies the measurement model (Equation 21) to:

$$\tilde{h}^b - \hat{\mathbf{C}}_b^{n,T} \tilde{h}^n = \hat{\mathbf{C}}_b^{n,T} \begin{pmatrix} h_e \\ -h_n \\ 0 \end{pmatrix} \gamma + \tilde{v}_m \quad (22)$$

## Inertial Sensor Setup

Addressing economic concerns, a reduction of inertial sensors would be possible depending on the application. **Table 1** provides a summary of various sensor setups and their corresponding outputs.

With a two-antenna GNSS compass, the roll angle is not observable. Nevertheless, for launcher applications, a two-antenna system is suitable since the roll angle is not necessarily of interest. In this case, the calculation of roll angles, and therefore the gyroscope in body-x direction, become dispensable. Furthermore, using tri-pods makes possible

Sensor setups in body coordinates	Prerequisite	Output
x-, y-, z-acc x-, y-, z-gyro	-	$\phi, \theta, \psi$
x-, z-acc y-, z-gyro	$\phi \approx 0$	$\theta, \psi$
z-gyro	$\phi \approx 0, \theta \approx 0$	$\psi$

TABLE 1. Sensor setups for different applications

a system structure alignment with a roll angle of zero degrees. Consequently, we expect no influence of the gravity vector on the body-y accelerometer measurement, which makes the corresponding sensor dispensable.

If only heading information is of interest, the body-y gyroscope becomes unnecessary. However, we note that an aiding of the LAMBDA method with pitch angle constraints would only apply to static pitch angles.

Finally, if a horizontally leveled system structure is guaranteed, it is justified to waive the remaining two accelerometers in the body-x and body-z directions, respectively. Deviations from the horizontal orientation of a few degrees are acceptable because these yield no essential decrease of yaw angle accuracy.

For launchers consisting of a tripod and a circular spirit level, the required alignment is readily accomplished. The Kalman filter state vector of such a system only includes two states, the yaw angle error  $\gamma$  and the error of body-z gyroscope bias estimate  $\Delta b_{\omega,z}$ , respectively. Accelerometer aiding is completely omitted.

### Multi-Sensor Compass

The fusion of the GNSS two-antenna system and the inertial attitude filter forms a coherent multi-sensor compass. Such a system has an increased availability and reliability compared to a pure GNSS compass as the inertial attitude information is used to reduce the ambiguity search space. Moreover, the newly formed compass is able to provide attitude information during GNSS signal outages.

We optimized our system for a portable launcher application. By using a tripod with a circular spirit level, the roll angle is approximately set to zero. Therefore, the appropriate inertial sensor setup consists of two gyroscopes (body-y and -z directions), two accelerometers (body-x and -z directions), and a magnetic field sensor.

The block diagram in **Figure 1** depicts the process of attitude determination. Double differences are built from carrier phase measurements of two GNSS receivers. Using these measurements, an estimation of the base vector,  $\vec{r}$ , as well as the vector of floating ambiguities,  $\vec{N}_{float}$  is carried out in an extended Kalman filter.

During operation the dynamic of a portable launcher only includes rotation motions. Therefore, the largest possible change of the base vector is caused by a rotation of 180 degrees, i.e., the position change is limited to twice the baseline length. Hence, for short baseline lengths, the simple discrete system model

$$\begin{pmatrix} \vec{r} \\ N_{float,1M} \\ \vdots \\ N_{float,nM} \end{pmatrix}_{k+1} = \begin{pmatrix} \mathbf{I} & \mathbf{0} \\ \mathbf{0} & \mathbf{I} \end{pmatrix} \begin{pmatrix} \vec{r} \\ N_{float,1M} \\ \vdots \\ N_{float,nM} \end{pmatrix}_k + \begin{pmatrix} \mathbf{I} \\ \mathbf{0} \end{pmatrix} \vec{\omega}_k \quad (23)$$

is suitable when changes of the base vector are accounted for by system noise,  $\vec{\omega}_k$ . The corresponding double-differenced mea-

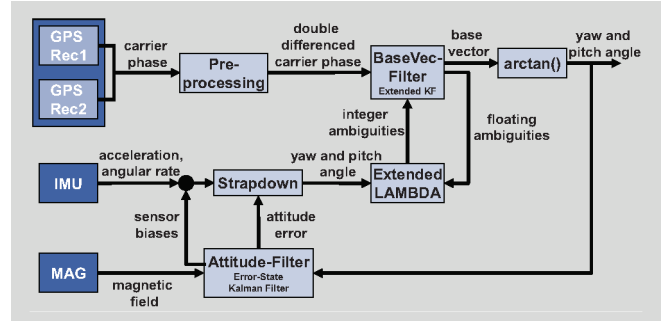


FIGURE 1 Block diagram of the integrated attitude system

surement model is given by:

$$\underbrace{\begin{pmatrix} \tilde{\phi}_{1M} \\ \tilde{\phi}_{2M} \\ \vdots \\ \tilde{\phi}_{nM} \end{pmatrix}}_{\tilde{y}} = \underbrace{\begin{pmatrix} (\vec{e}_1^T - \vec{e}_M^T) / \lambda & 1 & 0 & \dots & 0 \\ (\vec{e}_2^T - \vec{e}_M^T) / \lambda & 0 & 1 & \dots & 0 \\ \vdots & \vdots & \vdots & \dots & \vdots \\ (\vec{e}_n^T - \vec{e}_M^T) / \lambda & 0 & 0 & \dots & 1 \end{pmatrix}}_H \underbrace{\begin{pmatrix} \vec{r} \\ N_{float,1M} \\ \vdots \\ N_{float,nM} \end{pmatrix}}_{\tilde{x}} \quad (24)$$

where  $\vec{e}_j^T$  represents unit vector to the  $j$ th satellite,  $\vec{e}_M^T$  is the unit vector to the main satellite, and  $\lambda$ , the L1 wave length.

Using trigonometric transformation, we can extract a yaw and pitch angle solution from the base vector estimation.

Inputs of the LAMBDA algorithm consist of the floating ambiguity vector and the corresponding covariance matrix. Additionally, constraints on the baseline length, as well as the yaw and pitch angles, are provided for use in the extension of the LAMBDA method. As long as the integer ambiguities are not fixed, the LAMBDA method is invoked.

After successfully identifying all ambiguities, the vector of floating ambiguities,  $\vec{N}_{float}$  is eliminated from the state vector. From the known integer ambiguities,  $\vec{N}_{int}$ , real carrier phase pseudoranges are built:

$$\rho_j = \tilde{\phi}_{jM} - N_{int,jM} \quad (25)$$

Thus, the measurement model for fixed ambiguities holds:

$$\begin{pmatrix} \rho_1 \\ \rho_2 \\ \vdots \\ \rho_n \end{pmatrix} = \begin{pmatrix} (\vec{e}_1^T - \vec{e}_M^T) / \lambda \\ (\vec{e}_2^T - \vec{e}_M^T) / \lambda \\ \vdots \\ (\vec{e}_n^T - \vec{e}_M^T) / \lambda \end{pmatrix} \cdot \vec{r} \quad (26)$$

The attitude accuracy does not reach the required level until all ambiguities are fixed and consequently the estimation of the base vector is based on carrier phase pseudoranges.

### Measurement Results

In order to evaluate the performance of our system, several measurement campaigns were carried out on the roof of the Institute of Systems Optimization, Karlsruhe.

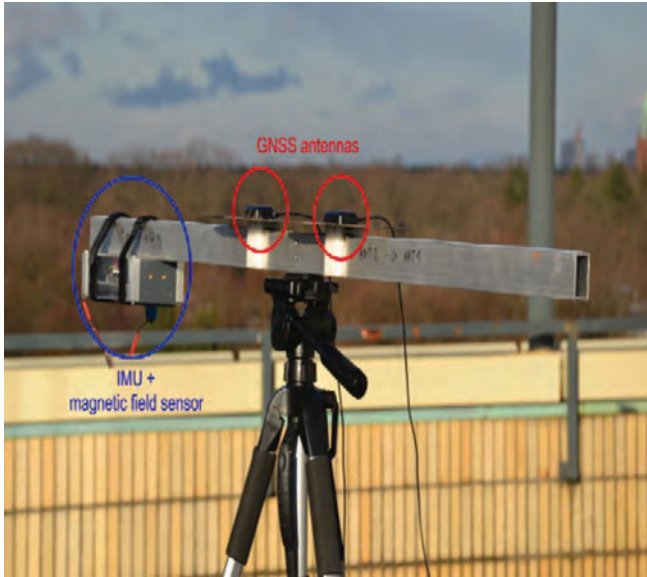


FIGURE 2 Test setup

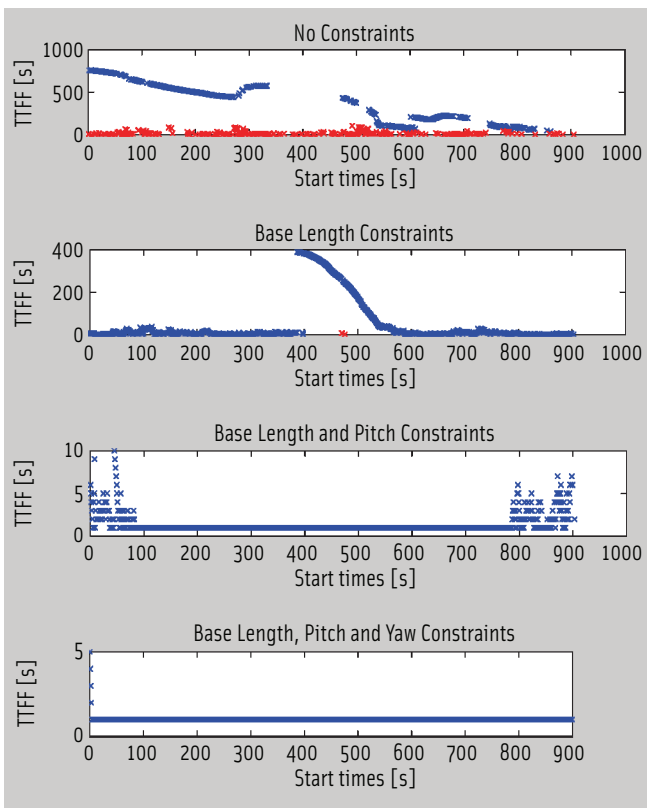


FIGURE 3 TTFF for static test

**Figure 2** shows the GNSS compass hardware setup, consisting of two single-frequency GNSS receiver sensor boards and two single-frequency patch antennas. For better reception, the antennas are attached on small ground plates. Our inertial attitude system is solely comprised of low-cost micro-electromechanical system (MEMS) components: gyroscopes, accelerometers, and a three-axis magnetic field sensor.

**Time to First Fix.** In the first static test, a baseline length of 20

Constraint tolerance	Mean TTFF [s]	Number Fixes	Number wrong fixes
-	228.97	700	423 (39,6%)
$\pm\Delta l = 5\text{cm}$	48.13	900	3 (0,3%)
$\pm\Delta l = 5\text{cm}$ $\pm\Delta\theta = 15^\circ$	1.37	900	0 (0%)
$\pm\Delta l = 5\text{cm}$ $\pm\Delta\theta = 15^\circ$ $\pm\Delta\psi = 30^\circ$	1.0155	900	0 (0%)

TABLE 2. TTFF statistics for static test

centimeters was used and the construction was approximately horizontally aligned. During a measurement campaign of 15 minutes, inertial data, and GNSS raw data were logged. During this initial time period, the GNSS compass was not rotated. We used offline processing to investigate the time to first fix (TTFF). In order to gain statistically sustainable results, a new filter was started with every GNSS epoch (one hertz) and the corresponding TTFF, recorded.

**Figure 3** depicts the results of the measurement campaign using various constraints. The upper plot is based on the original LAMBDA algorithm, which does not exploit any constraints. The average TTFF was about 230 seconds, whereas only 700 of a possible 900 fixes could be achieved during the 15-minute data-recording session. Moreover, almost 40 percent of the determined fixes were potentially wrong (points shown in red in Figure 3).

The indicator for incorrect fixes is derived from the baseline length that results from the respective integer ambiguities of the accepted fix. If this baseline length exceeds the true length by 10 percent or more, then the fix is presumably wrong. All of this reveals that the LAMBDA method is not convenient for GNSS compass applications.

The three lower plots in Figure 3 show the TTFF resulting from exploiting different constraints in the Extended LAMBDA method. Considering that the minimum possible TTFF is one second (one epoch), using constraints for the baseline length, the pitch, and yaw angles yields optimal results (cf. lower plot). All possible fixes were instantaneously calculated except for those of the first four seconds. However, these delays only occurred because the necessary number of satellites for starting the ambiguity identification process were not yet available.

A closer look at the statistics of this measurement campaign (see **Table 2**) illustrates that availability is not the only thing improved by using attitude constraints. The constraints also increase the reliability of heading information as incorrect fixes are prevented. Because use of constraints reduces the ambiguity search space, possible wrong combinations of ambiguities are excluded from the very beginning.

In a second campaign, the system was rotated around its vertical axis by hand. We attempted to induce different angular rates. The upper plot of **Figure 4** depicts the generated yaw angles over time extracted from the inertial attitude filter. These yaw angles are applied as constraints in the Extended LAMBDA method. Once again, we calculated the TTFF using

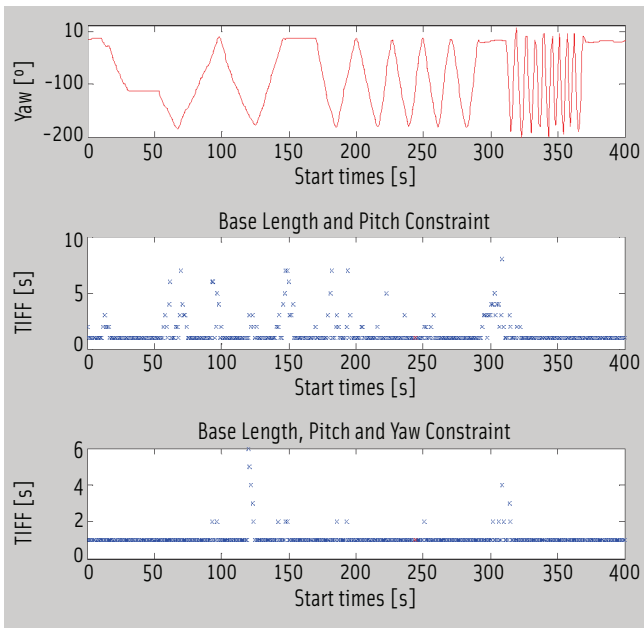


FIGURE 4 TTFF dynamic test

Constraint tolerance	Mean TTFF [s]	Number Fixes	Number wrong fixes
$\pm\Delta l = 5\text{cm}$ $\pm\Delta\theta = 30^\circ$	1.46	400	1
$\pm\Delta l = 5\text{cm}$ $\pm\Delta\theta = 30^\circ$ $\pm\Delta\psi = 45^\circ$	1.08	400	1

TABLE 3. TTFF statistics for dynamic test

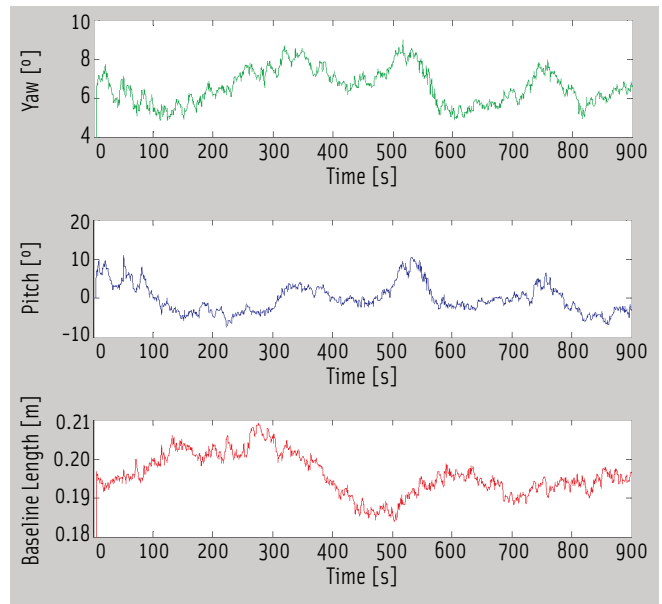


FIGURE 5 Solution accuracy for GNSS compass static test

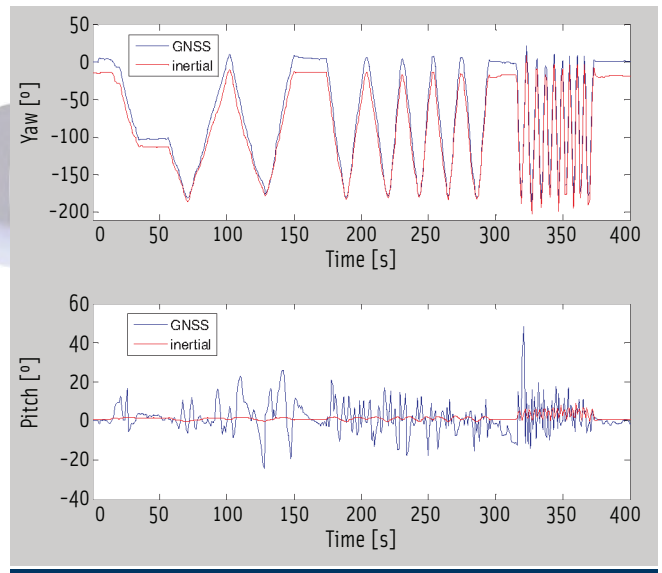


FIGURE 6 Yaw and pitch angle solution from GNSS and inertial filter

various attitude constraints. By applying all constraints, instantaneous fixing is achieved, except for just a few filter instances. The maximum TTFF is six seconds.

For the dynamic test, we increased the range of tolerance for attitude constraints, as seen in Table 3, because we wanted to avoid excluding the true ambiguities by selecting tolerances that are too small. Depending on the quality of redundant attitude information, ambiguity fixing can be postponed for a longer period of time.

**Accuracy.** Besides the capability of ambiguity fixing, the most important quality indicator for our system is the achievable heading accuracy. The major advantage of a GNSS heading system compared to an inertial system is that we should expect no offset. Hence, the accuracy of GNSS heading information can be assessed by static measurements. In principle, the accuracy decreases with smaller baseline lengths as errors in the estimated base vector yield larger attitude errors.

Compass solution	Mean	Standard deviation
Yaw	6.53°	1.02°
Pitch	-0.05°	3.60°
Baseline length	19.46 m	1.55 cm

TABLE 4. Solution averages for GNSS compass static test

Figure 5 depicts the solution of yaw and pitch angles over 15 minutes with a baseline length of 20 cen-

timeters. The standard deviation of the yaw and pitch angle is 1.02 and 3.6 degrees, respectively, as shown in Table 4. The maximum yaw angle error is below 2.0 degrees. The larger pitch angle error results from a well-known fact concerning all GNSS positioning solutions. Because of the geometric arrangements of satellites, horizontal positioning is much more accurate than vertical.

From Figure 5, we can see that the estimated base vector, and consequently the compass solutions, are subject to low- and high-frequency interference. While the high-frequency interference is caused by the thermal noise of the GNSS receivers, the low-frequency deviations arise from multipath effects.

Figure 6 shows the yaw and pitch angle solution of the dynamic test. At the beginning and at the end of the campaign,

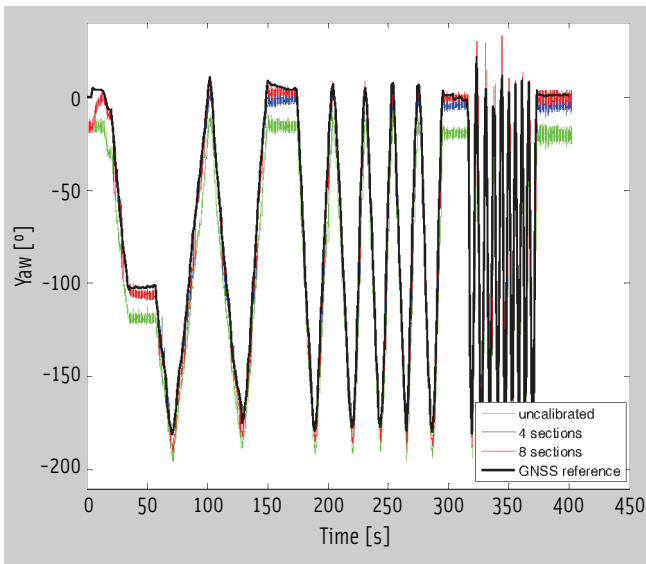


FIGURE 7 Online calibration of the magnetic field sensor

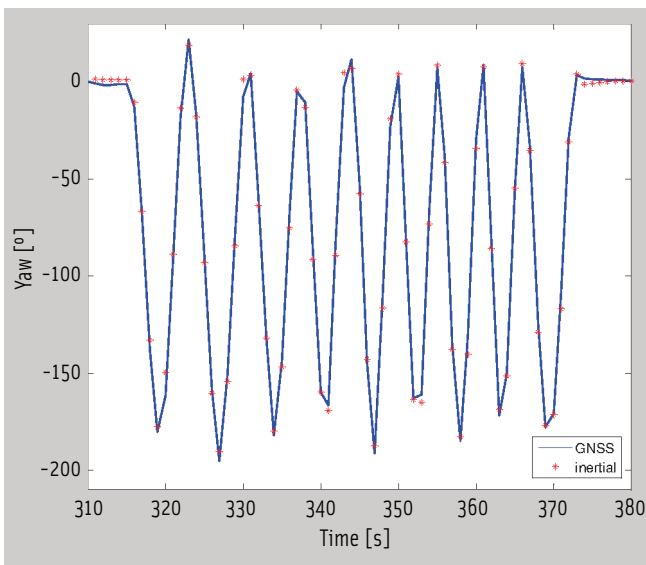


FIGURE 8 Inertial yaw angle for a calibrated system during GNSS dropout

the system was approximately aligned to the North. This is confirmed by the GNSS solution. The yaw angle at the end is about 0.8 degree. The estimated yaw angle from the inertial attitude filter, however, is obviously afflicted with an offset error of about 16 degrees caused by the erroneous magnetic field sensor aiding. Accordingly, the horizontal attitude solution from GNSS is generally preferable.

However, the situation is different for the pitch angle solution. While the GNSS accuracy is as yet comparable to the inertial solution for static situations, this is not the case for increasing dynamics. The standard deviation of the pitch angle solution for the GNSS and inertial filter is 7.6 and 1.0 degrees, respectively. This relation will not essentially change with increasing baseline length.

Dynamics exert great influence on the quality of carrier phase measurements, especially for low-cost receivers. There is a tradeoff between measurement noise and dynamic robustness. If the bandwidth of the phase lock loop in the receiver is large, measurement noise increases. On the other hand, for a lower bandwidth, the probability of losing track of the signal increases with occurring dynamics. Thus, unlike horizontal information, the pitch angle should be taken from the solution of the inertial attitude filtering.

## Model Refinements

Since a yaw angle aiding with accelerometer measurements is not possible, the accuracy of inertial yaw angle estimation depends on the quality of measurements from the magnetic field sensor. The integrity of those measurements, however, strongly depends on environmental conditions.

As can be seen from the plot in Figure 6, GNSS provides a much more reliable yaw angle solution. Hence, it is reasonable to replace the magnetic field measurement aiding for horizontal attitude with the GNSS yaw angle solution whenever available. Consequently, the magnetic field sensor is only required during GNSS outages.

**Online Calibration of the Magnetic Field Sensor.** In order to calibrate the magnetic field sensor, reference heading information is necessary. Thus, accomplishing an online calibration of the magnetic field sensor is possible as long as GNSS heading information is available. A way to do this is by modeling errors as bias and scale factors and computing them in an estimation process.

For a yaw angle extraction from magnetic field measurements, the actual magnetic field on the spot is required. This can be calculated from the WMM model; however, magnetic interference fields caused by metallic objects in the vicinity can yield locally limited deviations. Therefore, we based the calibration process of our system on another approach that is easy to implement and also accounts for those influences that are not measurement errors in a proper sense.

We begin our approach by dividing the measurement range into several sections. For every section the difference of the measurement and the expected measurement is accumulated. The calculated average value is used as a bias correction for each particular section.

The calibration results are shown in Figure 7. Here the data demonstrate that the initial bias error of almost 20 degrees is corrected within a few seconds. A classification of eight measurement sections is sufficient. A more refined classification does not offer further advantages.

With a calibrated magnetic field sensor, the quality of the inertial estimation of the yaw angle is comparable to the GNSS solution. Figure 8 depicts the inertial yaw angle during a simulated GNSS outage starting after 200 seconds. In the first 200 seconds, the magnetic field sensor is calibrated by means of the GNSS solution. Subsequently, the horizontal aiding changes from GNSS to magnetic field measurements without any loss of accuracy.

**Integrity Monitoring.** Due to the stochastic nature of measurement errors, incorrect fixes can never be completely excluded. On the basis of residual integrity monitoring, the detection of errors is only possible after several minutes when the direction to satellites has measurably changed. Additionally, false alarm should be avoided as no reliable GNSS solution is provided during the period of ambiguity fixing.

This article demonstrates that the time to first fix is greatly reduced by using the Extended LAMBDA method and constraints based on redundant attitude information. This enables a more sensitive integrity monitoring, because an immediate ambiguity fix is guaranteed.

Our method also provides new measurements for monitoring, namely, the given baseline length and the redundant attitude information. Therefore, in addition to the residual cycle slip detection for carrier phase measurements, a verification of the GNSS attitude solution based on fixed ambiguities is carried out. If the estimated baseline length differs more than 10 percent from the given baseline length, the current fix is rejected. The same applies for large deviations of GNSS attitude from inertial attitude.

**Conclusions**

In this article, a multi-sensor attitude system for portable, small-sized launcher applications was described. Accelerometers, gyroscopes, and a magnetic field sensor were combined with a GNSS compass. By using an extension of the LAMBDA method which accounts for baseline length and attitude constraints, an ambiguity resolution within a few epochs is guaranteed. The required redundant attitude information originates from a Kalman filter estimation based on inertial and magnetic field measurements.

The reduction of the ambiguity search space caused by exploiting attitude constraints not only results in shortening the time to first fix but also increases the reliability of the ambiguity resolution. Furthermore, the availability of a redundant attitude solution enables

bridging GNSS dropouts and enhanced integrity monitoring.

In order to improve the pure inertial attitude quality, an online calibration of the magnetic field sensor was implemented. The measurement results show that even for the short baseline length of 20 centimeters the maximum error of yaw angles is less than two degrees with a standard deviation of less than one degree.

**Acknowledgment**

This article is based on a paper presented at the 2012 ION International Technical Meeting.

**Manufacturers**

The GNSS compass hardware shown in Figure 2 consists of two Magellan AC12 GNSS receivers (subsequently a product of Ashtech, Inc., which was acquired by Trimble, Sunnyvale, California, USA) and two single-frequency ANN-MS-1-00 patch antennas from u-blox, Thalwil, Switzerland. Our inertial attitude system is solely comprised of low-cost micro-electro-mechanical (MEMS) components, namely ADIS 16255 gyroscopes from Analog Devices, Inc., Norwood, Massachusetts USA, SCA 3000 D01 accelerometers from Murata Electronics Oy (formerly VTI Technologies Oy, Vantaa, Finland), and an HMC 5843 three-axis magnetic field sensor from Honeywell, Inc., Plymouth, Minnesota, USA.

**Additional Resources**

- [1] Mönikes, R., and J. Wendel, J. and G. F. Trommer, "A Modified LAMBDA Method for Ambiguity Resolution in the Presence of Position Domain Constraints," *Proceedings of the 18th International Technical Meeting of the Satellite Division of The Institute of Navigation*, pages 81-87, 2005
- [2] Mönikes, R., and O. Meister, J. Wendel, and G. F. Trommer, "Yaw Angle Estimation of VTOL-UAVs with the Extended LAMBDA Method and Low Cost Receivers," *Proceedings of the 2007 National Technical Meeting of The Institute of Navigation*, pages 179-186, 2007
- [3] National Oceanic and Atmospheric Administration (NOAA): World Magnetic Model (WMM), <<http://www.ngdc.noaa.gov/geomag/WMM/>>, 2010

[4] Park, C., and P. Teunissen, "A New Carrier Phase Ambiguity Estimation for GNSS Attitude Determination Systems," *Proceeding of International Symposium on GPS/GNSS*, Tokyo, pages 283-290, 2003

[5] Teunissen, P., "The Least-Squares Ambiguity Decorrelation Adjustment: A Method for Fast GPS Integer Ambiguity Estimation," *Journal of Geodesy*, Vol. 70, No. 1, pp. 65-82, 1995

**Authors**



**Jochen Roth** is a Dr.-Ing. candidate at the Karlsruhe Institute of Technology, Germany. He received his Diploma in electrical engineering and information technology from the University of Karlsruhe. His primary research interests are GPS/INS integration with a focus on GNSS carrier phase processing and GNSS-based collaborative positioning.



**Claus Kaschwich** received his Diploma in electrical engineering and information technology from the Karlsruhe Institute of Technology. Currently, he is a Dr.-Ing candidate at the Technische Universität Braunschweig. His areas of research include navigation of unmanned aerial vehicles and prefiltering of inertial sensors.



**Gert F. Trommer** received the Dipl.-Ing. and the Dr.-Ing. degrees in electrical engineering from the Technical University of Munich, Germany. He joined EADS/LFK, formerly MBB/Dasa, where he was project manager for the IMU development in the UK ASRAAM program. He was director of the section "Flight Control Systems" with the responsibility for the navigation, guidance and control subsystem, the IR seeker. and the fin actuators in the German/Swedish Taurus KEPD 350 program. Since 1999 he has been a professor and director of the "Institute of Systems Optimization" at the Karlsruhe Institute of Technology, formerly University of Karlsruhe. His research focus is on guidance, navigation and control of dynamic mobile platforms. 



# TRANSFORM **THE WAY THE** WORLD WORKS



## Don't miss Trimble Dimensions 2012!

Join leaders in your industry at the premier conference for positioning professionals and learn first-hand what the future of positioning technology holds for you. Gain insight into how you can effectively leverage innovative solutions that are transforming the way the world works—from how highly integrated tools are changing the way surveying is performed to how construction projects are designed, executed and managed to how geospatial data is collected and analyzed for a wide range of applications.

Trimble Dimensions offers a wide range of educational and networking opportunities—with over 400 sessions from industry experts, inspirational keynote speakers, a pavilion showcasing the latest technologies, and special events to mingle with peers from around the world—learn how positioning technology is transforming the way the world works!

Register now at [www.trimbledimensions.com](http://www.trimbledimensions.com)

Trimble  
**DIMENSIONS** 2012

November 5-7 | The Mirage | Las Vegas  
[www.trimbledimensions.com](http://www.trimbledimensions.com)